Effects of Temperature, pH, and Salt Concentration on β-Lactoglobulin Deposition Kinetics Studied by Optical Waveguide Lightmode Spectroscopy

Marek Kroslak,[†] Jan Sefcik,*[,‡] and Massimo Morbidelli*[,†]

Institut für Chemie- und Bioinginieurwissenschaften, ETH Zürich, 8093 Zürich, Switzerland, and Department of Chemical and Process Engineering, University of Strathclyde, James Weir Building, 75 Montrose Street, Glasgow, G1 1XJ Scotland, United Kingdom

Received March 27, 2006; Revised Manuscript Received October 26, 2006

Deposition kinetics of β-lactoglobulin at a solid−liquid interface was studied with optical waveguide lightmode spectroscopy (OWLS) over a range of temperatures between 61 and 83 °C. A new temperature-controlled cell for OWLS measurements allows fast, on-line monitoring of the deposit formation at elevated temperatures. Primary protein layers were deposited at 25 °C in order to precondition and stabilize the waveguide surface. Sustained deposition lasting from a few minutes (around 80 °C) to hours (below 70 °C) resulted in multilayer deposits up to several tens of nanometers thick. The measured deposition rates were strongly influenced by temperature, pH, and NaCl concentration. Deposition rates decreased with increasing pH from 5.5. to 7.4, in a trend similar to that for noncovalent aggregation of β-lactoglobulin in solution. Activation energies for deposition rates decreased with increasing pH, from 340 kJ/mol at pH 5.5 to 230 kJ/mol at pH 7.4 and were similar to the activation energies for denaturation of β-lactoglobulin in solution.

1. Introduction

β-Lactoglobulin (β-LG) plays a crucial role during the heat treatment of milk. It is the main protein in whey, comprising approximately 50% of the total whey proteins in bovine milk. At room temperature and at pH values between 5.2 (the isoelectric point) and 7 it is well-soluble in water, where it exists mainly as a dimer stabilized by hydrogen bonds.[1] At these conditions β-LG spontaneously adsorbs on most surfaces from aqueous solutions, resulting in an irreversibly bound single-layer film. Further deposition on primary β-LG layers is very slow unless heat treatment is applied. At temperatures typical for milk processing (such as pasteurization) between 60 and 90 °C, voluminous deposits are rapidly formed at solid surfaces, leading to serious fouling problems. It is well-known that fouling phenomena at this range of temperatures are related to thermal denaturation of β-LG.[2]

During thermal exposure at pH values above the isoelectric point, the unfolding of the native globular structure exposes the hydrophobic region of β-LG, which contains disulfide bonds as well as one free thiol group.[3] Moreover, at pH values between 7 and 9 there is a gradual conformational change so that at pH 9 the thiol groups are exposed even at the ambient temperature.[4,5] As a consequence of this reversible unfolding, the chemical reaction of the thiol group with disulfide bonds results in protein aggregation and thus irreversible denaturation. In addition to the covalent bridging via disulfide bonds, there is also physical (noncovalent) aggregation due to exposure of the hydrophobic residues, resulting in a complex aggregation mechanism influenced by temperature, pH, salt concentration, surfactant presence, and protein concentration.[1,4,6−11]

* Authors to whom correspondence should be addressed. Phone: +44 141 5482410 (J.S.); +41 1 6323033 (M.M.). Fax: +44 141 5522302 (J.S.); +41 1 6321082 (M.M.). E-mail: jan.sefcik@strath.ac.uk; morbidelli@chem.ethz.ch.

[†] ETH Zürich.

[‡] University of Strathclyde.

Denaturation and aggregation of β-LG can thus be described in two successive yet interlinked steps. The first step is a reversible transformation between the protein native state and the unfolded state, where unfolding follows simple first-order kinetics. Upon unfolding the inert hydrophobic part and the thiol group are exposed and become reactive, which allows for irreversible denaturation of the unfolded protein to proceed. The second step is then aggregation of unfolded proteins through covalent (irreversible reaction of thiol groups) and noncovalent mechanisms resulting in protein denaturation. Kinetics of denaturation are usually experimentally determined by monitoring time evolution of the fraction of protein remaining in its native state. Depletion of the native protein concentration in time is customarily described in the literature[9,10,12,13] using the *n*th order kinetic expression

$$\frac{dN}{dt} = -k_{den}N^n \tag{1}$$

where N is the concentration of the native protein and k_{den} is the corresponding denaturation rate constant. Depending on the experimental conditions, the apparent reaction order n obtained by fitting experimental data was found to vary between 1 and 2. Since the overall process involves first-order unfolding followed by multiple reaction and aggregation steps, it is not surprising that a complex dependence of denaturation kinetics on temperature, pH, and protein concentration is observed.

The denaturation temperature of β-LG (i.e., the temperature where unfolding and subsequent depletion of the native form becomes observable) decreases from approximately 75 °C at pH ≈ 5 to 60 °C at pH ≈ 5, 50 °C at pH ≈ 8, and 25 °C at pH ≈ 9 .[1] Measured denaturation rates increase with increasing pH values between 5 and 8, while the activation energy corresponding to the denaturation rate constant in eq 1 decreases with increasing pH.[14] It was found that denaturation rates of β-LG are closely related to the availability and reactivity of

10.1021/bm060293+ CCC: $37.00
Published on Web 02/16/2007

the free thiol groups, which increase with pH,[15] so that denaturation kinetics are primarily driven by covalent bonding of unfolded proteins. However, formation of large β-LG aggregates as monitored by light scattering was found to be primarily driven by noncovalent physical aggregation. Kinetics of physical aggregation of β-LG become slower with increasing pH values between 5 and 8 due to the increasing negative charge of the protein as the pH is moving away from its isoelectric point.[15,16]

Although there have been numerous studies on thermal stability, aggregation, and fouling in β-LG solutions, there have been only a few experimental studies addressing the kinetics of early stages of β-LG deposition at solid surfaces at elevated temperatures. It was noted early on that the macroscopic fouling by β-LG becomes faster as pH is decreased from 7 to 5, opposite to the trend observed for β-LG denaturation, and it was suggested that the deposition kinetics of β-LG essentially follow its aggregation kinetics in the bulk.[17] Ellipsometry and reflectometry were used to study the early stages of deposition kinetics of β-LG on chromium oxide, stainless steel, and modified stainless steel surfaces. Elofsson et al.[18] studied deposition of a rather concentrated solution of β-LG (48 g/L) in phosphate buffer with 0.1 M NaCl at pH = 6.9 and temperatures of 65−68 °C on chromium oxide. Jeurnink et al.[2] used reflectometry to study the effects of preheating on deposition of whey protein isolates and β-LG at various concentrations in water at pH = 7.1 at temperatures of 70−95 °C on chromium oxide surfaces. Santos et al.[19] used ellipsometry to study the deposition of whey protein isolates at various concentrations in water at pH = 6.7 and 7.8 at temperatures of 85 °C. Variously modified stainless steel surfaces were used, including one with a sol−gel-based silica surface. They found that while most surface modifications did not change the deposition rate very much compared to the original stainless steel some modifications resulted in approximately 2-fold reduction in the long-term deposition rate, while the silica surface showed an approximately 2-fold increase. This also confirms that there is only a limited effect of the original surface properties on long-term fouling rates after a multilayer deposit is formed on the solid surface.

In this work we present measurements of heat-induced deposition rates of β-LG using optical waveguide lightmode spectroscopy (OWLS). OWLS belongs to a class of optical reflection techniques including also ellipsometry and reflectometry. It is an established technique to follow in situ adsorption and deposition at solid−liquid interfaces, especially for proteins at ambient temperature. We use OWLS to determine the kinetics of β-LG deposition at the silica−titania waveguide surface over a broad range of temperatures and pH values.

2. Methods

Optical waveguide lightmode spectroscopy is based on the change of the effective refractive index of an optical waveguide when a thin film forms at the waveguide surface. The presence of the thin film changes the evanescent electromagnetic field in close vicinity to the waveguide surface, and it affects the light reflection from the waveguide surface. This results in a shift of the incidence angle of a light beam leading to a lightmode guided along the waveguide. By measuring the incidence angle α corresponding to the resonance maximum of the light incoupled into the waveguide it is possible to determine an effective refractive index N of the light propagating along the waveguide as follows[20]

$$N = n_{\mathrm{air}} \sin \alpha + l\lambda_0/\Lambda \tag{2}$$

Here Λ is the grating period, l is the diffraction order ($l = 1$), λ_0 is the laser beam wavelength in vacuum, α is the incoupling incidence angle for the resonance maximum, and n_{air} is the refractive index of air. Under resonance conditions, the phase change that the electromagnetic wave undergoes during a round trip across the waveguide is equal to an integer multiple of 2π. By round trip we mean the reflection at the interface (F,C), between the liquid bulk (C) and the waveguide film (F), the crossing of the waveguide and then reflecting back at the opposite interface (F,S), i.e., the interface between the waveguide film (F) and its glass support (S). The zeroth-order mode equation for such a standing electromagnetic wave propagating indefinitely along an asymmetric planar waveguide is given by

$$0 = 2k_0 t_{\mathrm{F}} \sqrt{{n_{\mathrm{F}}}^2 - N^2} + \varphi_{\mathrm{F,S}} + \varphi_{\mathrm{F,C}} \tag{3}$$

The above equation gives a relation between the measured effective refractive index and the optogeometric parameters of the composite waveguide. Here $\varphi_{\mathrm{F,S}}$ and $\varphi_{\mathrm{F,C}}$ denote the phase shifts upon reflection from the waveguide surfaces, $k_0 = 2\pi/\lambda_0$, and n_{F} and t_{F} represent the refractive index of the waveguide film and its thickness, respectively. Assuming that all optical interfaces are abrupt and the layers are homogeneous and isotropic, eq 3 can be written for both the transverse electric (TE) and the transverse magnetic (TM) modes as follows

$$0 = k_0 t_{\mathrm{F}} \sqrt{{n_{\mathrm{F}}}^2 - N^2} - \arctan\left[\left(\frac{n_{\mathrm{F}}}{n_{\mathrm{S}}}\right)^{2\rho}\left(\frac{N^2 - {n_{\mathrm{S}}}^2}{{n_{\mathrm{F}}}^2 - N^2}\right)^{1/2}\right] - \arctan\left[\left(\frac{n_{\mathrm{F}}}{n_{\mathrm{C}}}\right)^{2\rho}\left(\frac{N^2 - {n_{\mathrm{C}}}^2}{{n_{\mathrm{F}}}^2 - N^2}\right)^{1/2}\right] \tag{4}$$

where $\rho = 0$ for the TE mode and $\rho = 1$ for the TM mode, n_{S} is the refractive index of the substrate (below the waveguide), and n_{C} is the bulk medium refractive index (above the waveguide). If we measure the effective refractive indices N(TE) and N(TM) in the absence of any additional layer at the waveguide surface and the refractive indices of both the substrate n_{S} and the cover medium n_{C} are known, then we can solve the two equations (eq 4 for TE and TM) to calculate the unknown waveguide refractive index and thickness, n_{F} and t_{F}.

When a thin film is present at the waveguide surface, its optical properties with respect to the reflected light can be represented by the excess polarization density γ.[21] The phase shift $\varphi_{\mathrm{F,C}}$ at the waveguide surface can also be expressed in terms of γ so that a generalized form of eq 4 is obtained,[22] accounting for the presence of the thin film. This equation is then solved for γ, resulting in the following

$$\gamma = \left(\frac{({n_{\mathrm{F}}}^2 - {n_{\mathrm{C}}}^2)}{({n_{\mathrm{F}}}^2 - N(\mathrm{TE})^2)}\right)^{0.5}\left(-k_0 t_{\mathrm{F}}({n_{\mathrm{F}}}^2 - N(\mathrm{TE})^2)^{0.5} + \arctan\left(\frac{(N(\mathrm{TE})^2 - {n_{\mathrm{C}}}^2)}{({n_{\mathrm{F}}}^2 - N(\mathrm{TE})^2)}\right)^{0.5} + \arctan\left(\frac{(N(\mathrm{TE})^2 - {n_{\mathrm{S}}}^2)}{({n_{\mathrm{F}}}^2 - N(\mathrm{TE})^2)}\right)^{0.5}\right) \tag{5}$$

The excess polarization density is related to the distribution of optical density at the interface[22]

$$\gamma = k_0 \int_0^\infty (\epsilon_{\|}(z) - \epsilon_0(z))\, \mathrm{d}z = k_0 \int_0^\infty ({n_{\mathrm{A}}}^2{}_{\|}(z) - {n_{\mathrm{C}}}^2(z))\, \mathrm{d}z \tag{6}$$

where the subscript || refers to the direction parallel to the waveguide surface and n_{A} is the refractive index of the adsorbed thin film. We note that the dielectric constant of the nonadsorbing medium is equal to the second power of its refractive index ($\epsilon = n^2$). In the case of optically homogeneous isotropic film the integral in the above equations simplifies to $M\, \mathrm{d}\epsilon/\mathrm{d}c$, i.e., the total mass deposited per unit area of the film multiplied by the derivative of the dielectric constant with respect to the mass concentration of the deposits. The corresponding value of

dϵ/dc applicable for various protein solutions and thin films is 0.527 cm^3/g.[23] We note that the value of dϵ/dc varies very little (less than 1%) with temperature between 25 and 80 °C. Therefore the deposited mass can be expressed for all temperatures considered here in terms of the excess polarization density γ as follows

$$M = \frac{\gamma}{k_0}\frac{\mathrm{d}c}{\mathrm{d}\epsilon} \tag{7}$$

Using eqs 5 and 7 we can calculate the deposited mass per surface area M from the experimentally measured value of N(TE).

3. Experimental Section

β-LG from bovine milk used in this study was from Fluka (β-lactoglobulin A and B, purity ~80%, lot no. 1087564). Protein solutions were prepared by proper addition of β-LG into 10 mM HEPES buffer from Acros Organics (lot no. A019289801). Buffers were adjusted to the target pH and salt concentration by NaOH and NaCl addition, respectively. Protein solutions were left to equilibrate for at least 2 h before being used or stored at 4 °C for a maximum of 3 days. Ultrapure water (Millipore, 18 MΩ) was used for solution preparation. All solutions were degassed under vacuum before use to reduce the creation of bubbles in the OWLS cell.

Deposition experiments were performed using the instrument OWLS 110 made by Microvacuum, Ltd., Budapest, Hungary, with the integrated temperature control unit OWLS TC. The OWLS waveguides (75% SiO_2, 25% TiO_2) were supplied by Microvacuum. The waveguide layer of thickness $t_F \approx 180$ nm and refractive index $n_F \approx 1.76$ (at 25 °C) is supported by a glass substrate of refractive index $n_S = 1.52578$ with dimensions 12 mm × 8 mm × 0.5 mm. The waveguides were stored in a NaOH solution at pH = 11 for 3 h to uniformly activate hydroxyl groups on the surface prior to protein deposition. They were subsequently rinsed with water and dried with nitrogen. The waveguide was placed adjacent to the flow-through cell in the shape of a rectangular channel (8 mm long, 0.8 mm high, 2 mm wide) with a total volume of 12.8 μL, with entrance and exit ports. All delivery tubes and the measuring cell were made of Teflon.

Prior to the β-LG deposition, a buffer solution was flowed through the deposition cell, and the waveguide parameters were determined. The flow rate was held constant at 2 mL h^{-1} (corresponding to a residence time of approximately 30 s in the deposition cell) by the programmable syringe pump Vit-Fit (Lambda, Czech Republic). The syringe pump provided steady injection of the sample without flow rate pulses, which is particularly important for temperature measurements, because fluctuating flow rates induce oscillations of the fluid temperature, resulting in substantial noise in the experimental data. The response of the bare waveguide at elevated temperature was recorded prior to the deposition measurements.

4. Results and Discussion

4.1. Primary Layer Creation at Ambient Temperature. Primary exposure of oxide surfaces to protein solutions typically leads to spontaneous adsorption of thin protein layers. In this work, bare silica−titania waveguides were first equilibrated at 25 °C with the blank buffer solution at a flow rate of 2 mL h^{-1}. Then the waveguide was exposed to a β-LG solution in 10 mM HEPES, pH 5.5, at the standard flow rate for 60 min to create a primary protein layer. In Figure 1 we show the time evolution of the deposited mass of β-LG on the bare waveguide surface for two subsequent exposures to a 0.5 mg mL^{-1} solution of β-LG followed by rinsing with the blank buffer.

The first exposure to the β-LG solution for 60 min resulted in a total primary layer coverage of 1.4 mg m^{-2}. After reaching this coverage further growth of deposited mass becomes very slow. Subsequent desorption in the blank buffer for 60 min resulted in a decrease of the deposited mass to 0.7 mg m^{-2}. The subsequent exposure to the same β-LG solution for another 60 min resaturated the surface to the same total coverage as observed in the first exposure. Also, the second desorption resulted in the same deposited mass as in the first desorption. This mass of 0.7 mg m^{-2} corresponds to the irreversible primary layer, where the protein is irreversibly bound to the waveguide surface so that it cannot be removed from the surface by desorption in the blank buffer at 25 °C.

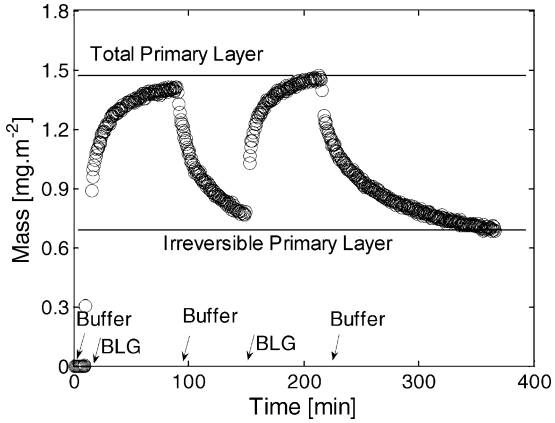

Figure 1. Primary exposure of bare waveguide to 0.5 mg mL^{-1} β-LG in 10 mM HEPES, pH 5.5, at 25 °C. Arrows above the time axis indicate change in the liquid phase.

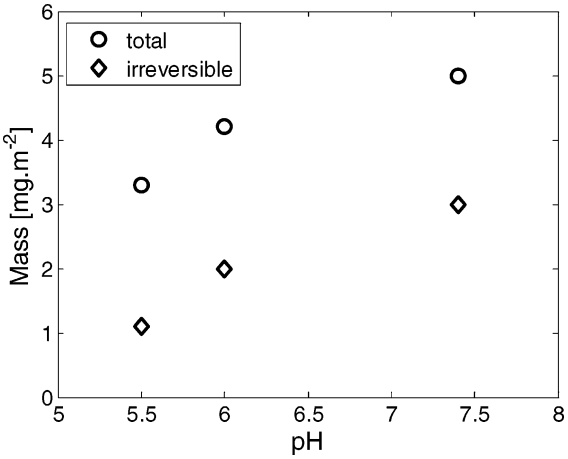

Figure 2. Effect of pH on total deposited mass (circles) and irreversibly deposited mass (diamonds): 10 mg mL^{-1} β-LG in 10 mM HEPES at 25 °C.

The density of the primary layer depends on various factors such as pH, salt concentration, protein concentration, and surface properties. We examined the effect of solution pH on the primary layer deposition from 10 mg mL^{-1} β-LG in 10 mM HEPES for the range of pH 5.5−7.4. Experiments showed the same deposition pattern as discussed in Figure 1, i.e., alternating between the total primary layer coverage and the irreversible primary layer coverage, as for the 0.5 mg mL^{-1} β-LG solution discussed above. The values of the mass corresponding to the total primary layer coverage after 1 h of deposition at ambient temperature as well as to the irreversible primary layer coverage after 1 h of rinsing with the buffer are shown in Figure 2 as a function of pH.

The observed adsorption behavior of β-LG is consistent with the classical protein deposition mechanism.[24,25] The adsorbed protein is present in two states: one irreversibly and the other reversibly adsorbed. Proteins slowly undergo conformational

Table 1. Refractive Indices as a Function of Temperature

parameter	25 °C	T (°C)	source
$n_{C,water}$	1.331144	$n^{25°C}_{C,H_2O} - \frac{75453.41\Delta T + 2340.431\Delta T^2 + 6.363191\Delta T^3}{T10^7 + 65.7081 \times 10^7}$ where $\Delta T = T - 25$	*a*
$n_{C,HEPES}$	1.333699	$1.33156 - 5.89189 \times 10^{-5}\, T - 1.06617 \times 10^{-6}\, T^2$	*b*
n_S	1.52571	$1.52542 - 1.23 \times 10^{-6}\, T$	*a*

[a] Reference 26. [b] Reference 32.

Table 2. Experimental Procedure for Temperature Exposure of Primary Protein Layers at 72 °C Shown in Figure 4

period	time (min)	bulk solution	flow rate (mL h^{-1})	temperature (°C)
A	0−81	buffer	2	25
B	81−89	buffer	2	heating
C	89−112	buffer	2	72
D	112−129	buffer	2	cooling
E	129−163	buffer	2	25
F	163−230	β-LG in buffer	2	25
G	230−400	buffer	2	25

changes after being adsorbed on oxide surfaces, and these changes result in a stronger interaction between the protein and the surface. Such strongly bound proteins loose their native structure and spread in time over the surface, thus hindering further protein irreversible deposition. Reversibly bound proteins are weakly attracted to the surface, which results in their accumulation at the interface, but they can be relatively easily removed by washing.

4.2. Deposition at Elevated Temperatures.

4.2.1. Temperature Response of the Bare Waveguide in Pure Buffer. Exposure of the bare waveguide to aqueous solutions at various temperatures leads to changes of the measured incoupling angle α and the corresponding effective refractive index N. This is due to the temperature dependence of the system optogeometric parameters: refractive indices of the substrate n_S and cover medium n_C as well as the thickness t_F and refractive index n_F of the waveguide itself. We can calculate the waveguide parameters t_F and n_F as a function of temperature from eq 4 for the TE and TM modes, using the measured values of N(TE) and N(TM) at the corresponding temperatures. The expressions used to describe the temperature dependence of n_S (glass substrate) and n_C (10 mM HEPES solution at pH = 7.4 and water) are reported in Table 1. It is worth noting that calculations of the deposited mass using the cover medium refractive index either for HEPES ($n_{C,HEPES}$) or for water ($n_{C,water}$), shown in Table 1, resulted in virtually identical results. This means that for the diluted aqueous solutions used here the OWLS response, eq 4, is insensitive to changes of n_C due to the cover medium composition.

The temperature response of the bare waveguide was measured in the presence of the buffer solution (10 mM HEPES, pH 5.5). Flow rate through the heated deposition cell was kept constant at 2 mL h^{-1}. The set of two nonlinear eqs 4 for the TE and TM modes was solved to obtain the waveguide parameters t_F and n_F, using the values of n_C and n_S in Table 1. The values of t_F and n_F measured at steady temperatures were fitted as a function of temperature T (in °C) using the following expressions, and the corresponding results are shown in Figure 3

$$t_F(T) = 184.31 + 0.0096872T - 9.5054 \times 10^{-6}T^2$$

$$n_F(T) = 1.7881 - 2.7434 \times 10^{-5}T - 2.2582 \times 10^{-7}T^2 \quad (8)$$

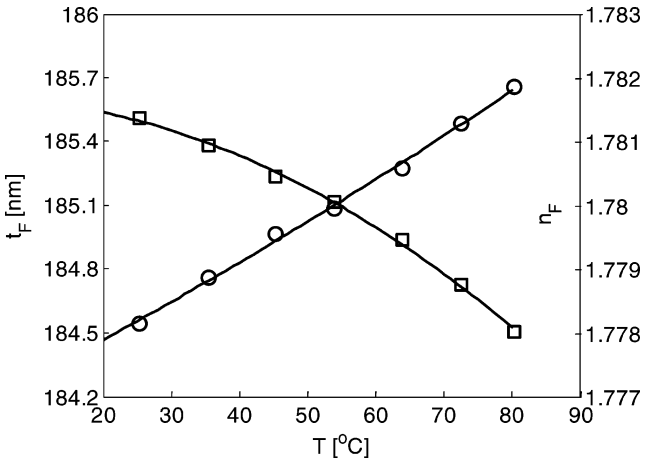

Figure 3. Waveguide parameters measured in 10 mM HEPES, pH 5.5, as a function of temperature. Circles represent the measured thickness t_F, and squares the refractive index n_F. Lines represent the fit given by eq 8.

A similar magnitude of the change in the waveguide thickness and refractive index with temperature was also measured in the presence of pure water, in agreement with previously published results.[26] It was proposed that the observed change in optogeometric parameters of the waveguide with temperature is caused by thermal expansion of the porous oxide constituting the waveguide.[26] The thermal expansion of the waveguide results in increasing thickness and therefore porosity with temperature, leading in turn to the decreasing refractive index of the waveguide.

When the waveguide was cooled back to ambient temperature, a change of approximately $\Delta n_F = 1 \times 10^{-3}$ in the waveguide refractive index was consistently observed for several waveguides exposed to the HEPES solution at pH values between 5.5 and 7.4. This change was significantly higher than the typical uncertainty in the optogeometric parameters (2×10^{-4} for n_F and 0.25 nm for t_F) determined from repeated experiments for a given waveguide. In all cases the temperature response of the bare waveguide to the buffer solution revealed gradual modification of the waveguide optical properties at elevated temperatures. The observed drift in the waveguide refractive index may be due to gradual hydrolysis of metal−oxide−metal bonds of metal (silicon and/or titanium) oxide interfaces in internal waveguide pores when exposed to aqueous solutions at elevated temperatures. Hydrolysis of metal−oxygen−metal bonds results in formation of highly polarizable metal−hydroxy groups, which then contribute to increasing the overall waveguide refractive index n_F.[33] The same effect was also observed for silica- and niobia-coated waveguides. Coating of waveguide surfaces (i.e., by polymer or protein) can be used to effectively suppress this effect by providing a barrier between the waveguide and the liquid solution and thus slowing down the waveguide hydrolysis. In particular, a primary protein layer adsorbed at ambient temperature can stabilize the waveguide at elevated temperatures, as will be discussed shortly.

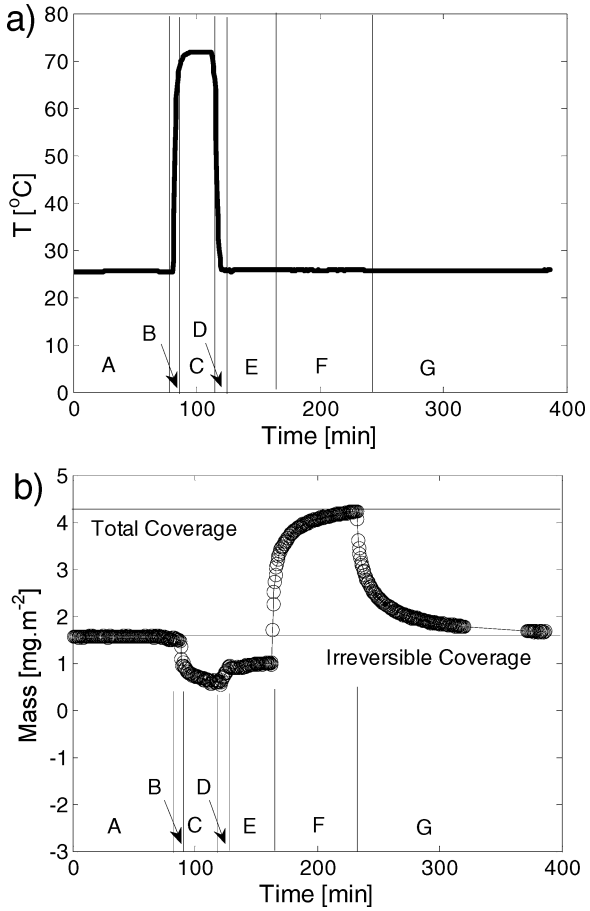

Figure 4. Temperature exposure of the thin protein layer in 10 mM HEPES solution, pH 5.5, at 72 °C. a) Temperature in deposition cell; b) deposited mass. The protein layer was resaturated with a 10 mg mL^{-1} β-LG solution.

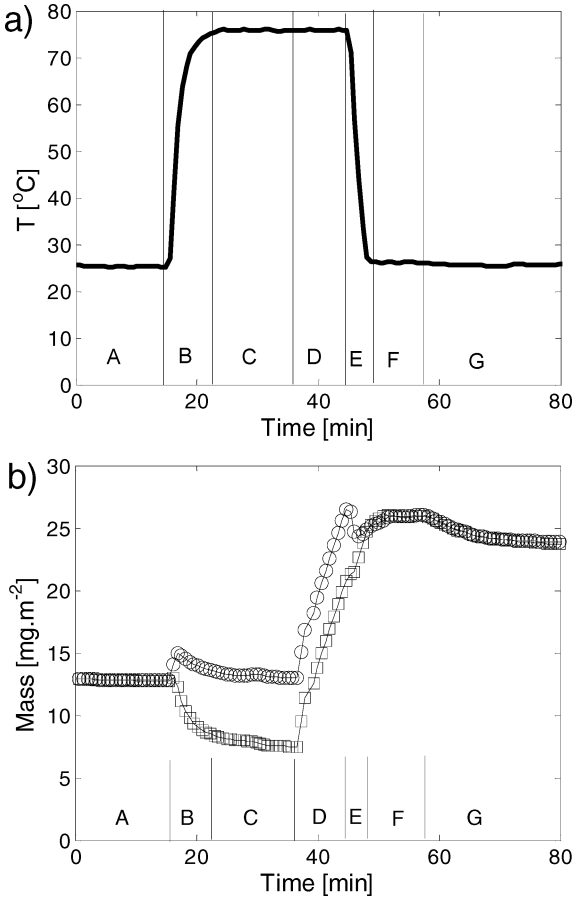

Figure 5. Secondary deposition from a 10 mg mL^{-1} β-LG solution at pH 5.5 and 75 °C on a previously deposited protein layer. a) Temperature in deposition cell; b) deposited mass. Values were computed with temperature correction for the optical properties (circles) and without correction (squares).

4.2.2. Temperature Stability of Primary Protein Layers in Pure Buffer. Before discussing thermally driven deposition of β-LG, we address the issue of durability of irreversibly bound primary protein layers deposited at ambient temperature when exposed to the buffer solution at elevated temperatures. A typical experiment is shown in Figure 4, starting with the protein layer deposited at 25 °C from a 10 mg mL^{-1} β-LG solution. The detailed experimental conditions are summarized in Table 1. At ambient temperature the irreversibly deposited protein amount was 1.6 mg m^{-2} (period A). After 30 min of heat treatment at 72 °C in 10 mM HEPES solution at pH 5.5 (period C) and cooling back to ambient temperature (period D), the measurement becomes steady at the end of period E. Here, the layer exhibits a partial loss of deposited mass, being the protein coverage decreased to 1.0 mg m^{-2}. Subsequent resaturation of the protein layer by native β-LG solution for 60 min (period F) at ambient temperature resulted in the complete recovery of the total coverage (4.2 mg m^{-2}) reached in the saturation step at ambient temperature (not shown in Figure 4) preceding the heat treatment. Subsequent rinsing with the blank buffer (period G) resulted in the recovery of the same irreversible coverage (1.6 mg m^{-2}) as observed before the thermal treatment.

The same observation was made for repeated thermal exposures of the same deposited protein layer at six different temperatures between 60 and 80 °C. Irreversibly deposited amounts measured before temperature exposure (period A) and at the end of buffer washing (period G) were always very similar (difference ±20%). These experiments showed that the protein layer, which partially degrades during the thermal treatment, can be fully recovered by subsequent resaturation at ambient temperature. Moreover, it has been observed that the optical properties of the waveguide covered by the primary protein layer are stable in the buffer solution at the temperatures considered in this work. Since this was not the case for bare surfaces as mentioned above, it is apparent that the protein layer effectively protects the waveguide beneath it from heated buffer solutions.

4.2.3. Secondary Deposition of β-LG on Thin Protein Layers at Elevated Temperatures. As discussed above, the first step in the β-LG deposition process is the formation of a primary layer, which occurs spontaneously even at ambient temperature. This primary layer is irreversibly bound to the original surface of the sensor, resulting in a significant modification of its surface properties. Further deposition at elevated temperatures is then essentially driven by interactions between the deposited proteins and the proteins in the bulk. To decouple the interaction between surface−protein (initial deposition) and protein−protein (secondary deposition) we measured the secondary deposition rates always starting with a protein layer several nanometers in thickness. In Figure 5 we show results from a typical secondary deposition experiment from a 10 mg mL^{-1} β-LG solution at 75 °C. The detailed experimental conditions are reported in Table 3. A previously deposited layer (13 mg m^{-2}) was present on the top of the waveguide (period A), so the influence of the original waveguide surface on the deposition rate is expected to be negligible. After the system was heated to the desired temperature (periods B and C), the β-LG solution was injected. After a very short transition time (in this case approximately 1 min) the rate of change of the deposited mass became constant,

Table 3. Experimental Procedure for Secondary Deposition Experiment at 75 °C Shown in Figure 5

period	time (min)	bulk solution	flow rate (mL h^{-1})	temperature (°C)
A	0−15	buffer	2	25
B	15−22	buffer	2	heating
C	22−36	buffer	2	75
D	36−45	β-LG in buffer	2	75
E	45−48	buffer	0	cooling
F	48−57	buffer	0	25
G	57−80	buffer	2	25

and the deposition rate at the given temperature could be determined from the slope of the linear growth observed in period D.

It is worth noting that the deposited mass shown by the circles in Figure 5 was calculated using the temperature correction of the optical properties described above in section 4.2.1 using the temperature measured on-line by a thermocouple located close to the deposition cell. It can be seen that the apparent deposited mass with temperature correction exhibits a small peak soon after the temperature started to increase at the beginning of period B. By the time the system reached a steady temperature (period C), this transient effect disappeared. This is an artifact due to the fact that in the non-steady-state regime the temperature measured by the thermocouple does not correspond to the real waveguide temperature. Therefore, the temperature correction used in period B of the experiment does not accurately represent the optical parameters of the system, and incorrect values of the deposited mass are obtained.

For the sake of illustration, the squares in Figure 5 show the values of the deposited mass calculated without applying the temperature correction. In this case, the calculated apparent deposited mass is significantly lower than the actual one represented by the circles in the same figure. However, the deposition rates (corresponding to the slope in period D) determined from the data calculated with and without temperature correction are very similar.

It is worth noting that an alternative simplified approach to the evaluation of the deposition rates can be used, based on treating the previously deposited layer of protein as part of the waveguide. In this case, apparent optogeometric parameters of the so-modified waveguide (consisting of waveguide and thin protein layer) n_F and t_F are determined using eq 4 at the relevant deposition temperature just before the injection of β-LG. We have seen that this approach yields deposition rates very similar to those of the more rigorous one based on the temperature correction of the waveguide parameters.

The values of mass deposited during the secondary deposition from 10 mg mL^{-1} β-LG solution (10 mM HEPES, pH 6.4) at various temperatures are shown in Figure 6 as a function of time. The deposition below 60 °C was so slow that it was not detectable with our instrumentation. The linearity of the mass growth in time was confirmed by long experiments lasting up to 2 h. These long experiments were performed for conditions where the deposition rate is slow enough so as to avoid the saturation of the waveguide evanescence region, which occurs at mass coverage of approximately 35 mg m^{-2}.

The deposition rates were found to increase exponentially with the temperature over the range of temperatures considered here. They were highest at pH 5.5 (close to the isoelectric point of β-LG) and decreased as pH was increased from 5.5 to 7.4. This pattern of dependence on pH is consistent with the trend observed for the growth of large aggregates in β-LG solutions.[5,27] When pH is above the isoelectric point of β-LG, increasing pH results in increasing negative charge on β-LG, which implies increasing electrostatic repulsion and thus slowing down of aggregation as well as deposition kinetics.

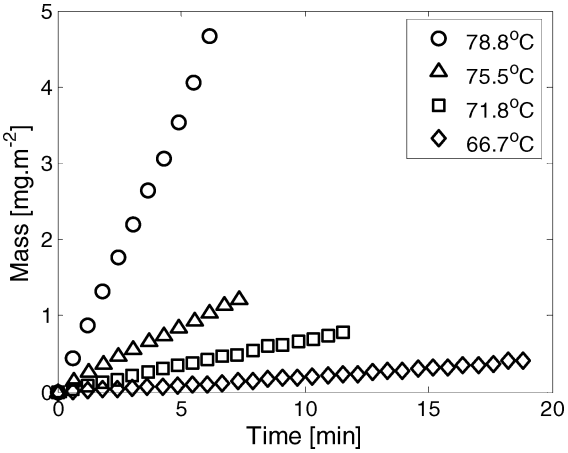

Figure 6. Growth of protein mass during secondary deposition from a 10 mg mL^{-1} β-LG solution in 10 mM HEPES at pH 6.4 and various temperatures.

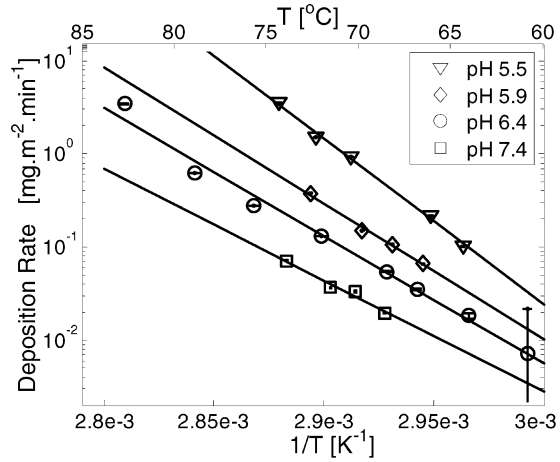

Figure 7. Arrhenius plot for the deposition rate from a 10 mg mL^{-1} β-LG solution in 10 mM HEPES. Points are the experimental values, the solid lines represent the linear fit.

It is worth noting that the residence time of the protein inside the deposition cell at elevated temperature is approximately 30 s. On the basis of previous experimental studies on β-LG aggregation[10] it is expected that growth of protein aggregates due to noncovalent (physical) aggregation is not significant for such short times, especially at higher pH (i.e., higher charge and thus stronger electrostatic repulsion) and lower temperatures (i.e., slower denaturation). However, at higher pH values and higher temperatures (where denaturation is faster), formation of small covalently bound clusters observed in bulk solutions[10] cannot be excluded before proteins are transported to the surface.

In Figure 7 we show the Arrhenius plots for secondary deposition rates at various pH values. From these the activation energy E_a for the secondary deposition process can be estimated, and the obtained values are shown in Figure 8 as a function of pH. These activation energies for β-LG deposition are similar to those previously reported for β-LG denaturation at comparable pH values found in the literature.[1,5,11,14] However, the denaturation kinetics become faster as pH increases,[4,5,28,29] which is opposite to the trend observed here for the deposition kinetics.

A possible explanation for the observed dependence of deposition rates and activation energies on pH is as follows.

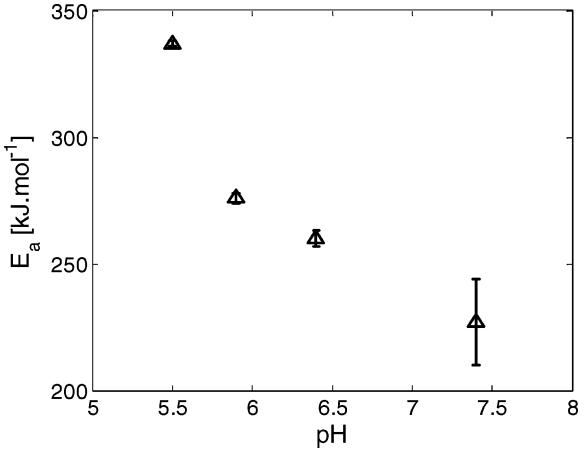

Figure 8. pH dependence of the activation energy for β-LG deposition.

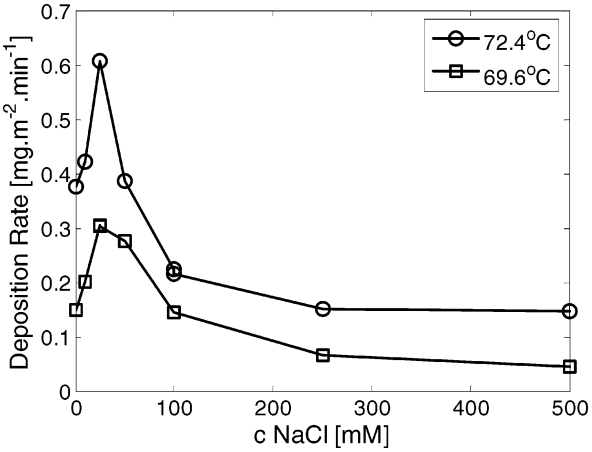

Figure 9. Deposition rates as a function of NaCl concentrations at two temperature values: 10 mg mL^{-1} β-LG solution in 10 mM HEPES at pH 5.9.

Let us consider that the deposition process consists of two steps in a series. Unfolding and denaturation of β-LG (facilitated by covalent binding of unfolded proteins) with the denaturation kinetics according to eq 1 with rate constant k_{den} are followed by deposition of denatured β-LG, with first-order kinetics and the deposition rate constant k_{dep}. Assuming that the conversion of the native protein is quite small within a short residence time in the deposition cell so that the extent of both the denaturation reaction and the subsequent deposition step stays small (i.e., only a small proportion of protein denatures and only a small proportion of denatured protein is deposited), it is easy to see that the overall rate of β-LG deposition R_{dep} would be proportional to the product of the two rate constants k_{den} and k_{dep}. Let us now consider the two rate constants written as the usual Arrhenius-type expression

$$k_{den} = {k_{den}}^0 \, e^{-E_a^{den}/kT}$$
$$k_{dep} = {k_{dep}}^0 \, e^{-E_a^{dep}/kT} \quad (9)$$

where k^0 and E_a are corresponding prefactors and activation energies, respectively. The overall rate of deposition R_{dep} is then proportional to

$$k_{den}k_{dep} = {k_{den}}^0{k_{dep}}^0 \, e^{-(E_a^{den}+E_a^{dep})/kT} \quad (10)$$

Now we can see that the activation energy corresponding to the deposition rates observed in our experiments is actually the sum of the two activation energies for the denaturation and the deposition step of the denatured proteins. However, the prefactor is given by the product of the two prefactors for the two steps. If the activation energy for denaturation is much larger than the activation energy for deposition of denatured protein, then the activation energy of the overall deposition step will be close to the activation energy for denaturation, as observed in our experiments. This is a reasonable assumption, since typical energy barriers for reaction-limited aggregation of charge stabilized colloids are not more than $10-20kT$,[30] which translates into anactivation energy of 25−50 kJ/mol, which is only approximately 10−20% of the activation energy values for the deposition rates in Figure 8. However, if the prefactor for the denaturation rate constant increases moderately with pH, while the prefactor for the deposition rate constant of denatured proteins decreases strongly with pH (as expected for aggregation in the reaction-limited aggregation regime[30]), then the prefactor for the deposition rate given by the product of the two decreases with pH, as observed in our experiments. It can then be concluded that the activation energy for the overall deposition rate follows the trend of the activation energy for denaturation, i.e., decreases with increasing pH, while the deposition rate follows the trend opposite to that of denaturation but consistent with aggregation, i.e., decreasing with increasing pH.

Finally, we analyze the effect of salt concentration on the deposition kinetics of β-LG. In Figure 9 we show the measured deposition rates as a function of NaCl concentration for two temperature values. A maximum in the deposition rate was observed at a concentration of the NaCl in the 10 mM HEPES buffer equal to approximately 30 mM. After the maximum is reached, the deposition rate decreases when further increasing the salt concentration. This qualitative behavior follows the well-known pattern of protein solubility in electrolyte solutions.[1] In general, the salt concentration influences both steps described in the deposition mechanism above. The observed maximum is caused by the combined effect of a reduced denaturation rate and an increased aggregation rate that follow an increase in salt concentration. NaCl belongs to the salting-out class of salts and thus stabilizes the native protein conformation, thus decreasing the denaturation rate.[31]

However, when the salt concentration is increased the charge of the protein is screened, and therefore the noncovalent aggregation is enhanced. Thus the maximum in the overall deposition rate with increasing NaCl concentration, observed in Figure 9, is related to the simultaneous decrease in the rate of the denaturation reaction and increase in the rate of aggregation.

5. Conclusions

Deposition of thin β-LG layers at the surface of silica−titania waveguides was monitored on-line by OWLS, an optical reflection technique related to ellipsometry and reflectometry. This is the first time that OWLS was used to quantitatively monitor the kinetics of temperature-driven deposition. The initial step in β-LG deposition is the primary coverage of the bare surface, which is partially reversible at ambient temperature. Primary coverage density at ambient temperature depends on β-LG concentration and pH. The irreversibly bound part of the primary layer is partially desorbed when exposed to pure buffer at elevated temperatures but can be resaturated to its original density from the protein solution at ambient temperature. The temperature-driven secondary deposition of β-LG is strongly

dependent on temperature and pH. Deposition rates were decreasing with increasing pH from 5.5. to 7.4 in a trend similar to that for noncovalent aggregation of β-LG in the bulk solution. Activation energies for deposition rates were decreasing with increasing pH, from 340 kJ/mol at pH = 5.5 to 230 kJ/mol at pH = 7.4, and were similar to the activation energies for denaturation of β-LG in the bulk solution. This is consistent with the fact that protein deposition is the result of two processes occurring in a series, protein denaturation followed by deposition of the denaturated protein. The effect of NaCl concentration on the deposition rate at elevated temperatures follows the inverse of a well-known pattern of protein colloidal stability, with a maximum deposition rate at moderate salt concentrations.

References and Notes

(1) Relkin, P. Thermal unfolding of β-lactoglobulin, α-lactalbumin, and bovine serum albumin. A thermodynamic approach. *Crit. Rev. Food Sci. Nutr.* **1996**, *36*, 565−601.

(2) Jeurnink, T. J. M.; Walstra, P.; deKruif, C. G. Mechanisms of fouling in dairy processing. *Neth. Milk Dairy J.* **1996**, *50*, 407−426.

(3) Laligant, A.; Dumay, E.; Valencia, C. C.; Cuq, J. L.; Cheftel, J. C. Surface hydrophobicity and aggregation of β-lactoglobulin heated near neutral pH. *J. Agric. Food Chem.* **1991**, *39*, 2147−2155.

(4) Monahan, F. J.; German, J. B.; Kinsella, J. E. Effect of pH and temperature on protein unfolding and thiol/disulfide interchange reactions during heat-induced gelation of whey proteins. *J. Agric. Food Chem.* **1995**, *43*, 46−52.

(5) Liu, T. X.; Relkin, P.; Launay, B. Thermal-denaturation and heat-induced gelation properties of β-lactoglobulin. Effects of some chemical parameters. *Thermochim. Acta* **1994**, *246*, 387−403.

(6) Baussay, K.; Le Bon, C.; Nicolai, T.; Durand, D.; Busnel, J. P. Influence of the ionic strength on the heat-induced aggregation of the globular protein β-lactoglobulin at pH 7. *Int. J. Biol. Macromol.* **2004**, *34*, 21−28.

(7) Pouzot, M.; Durand, D.; Nicolai, T. Influence of the ionic strength on the structure of heat-set globular protein gels at pH 7. β-Lactoglobulin. *Macromolecules* **2004**, *37*, 8703−8708.

(8) Tobitani, A.; Ross-Murphy, S. B. Heat-induced gelation of globular proteins. 1. Model for the effects of time and temperature on the gelation time of BSA gels. *Macromolecules* **1997**, *30*, 4845−4854.

(9) Kessler, H. G.; Beyer, H. J. Thermal denaturation of whey proteins and its effect in dairy technology. *Int. J. Biol. Macromol.* **1991**, *13*, 165−173.

(10) Le Bon, C.; Nicolai, T.; Durand, D. Kinetics of aggregation and gelation of globular proteins after heat-induced denaturation. *Macromolecules* **1999**, *32*, 6120−6127.

(11) Sava, N.; Van der Plancken, I.; Claeys, W.; Hendrickx, M. The kinetics of heat-induced structural changes of β-lactoglobulin. *J. Dairy Sci.* **2005**, *88*, 1646−1653.

(12) Anema, S. G. Effect of milk concentration on the irreversible thermal denaturation and disulfide aggregation of β-lactoglobulin. *J. Agric. Food Chem.* **2000**, *48*, 4168−4175.

(13) Galani, D.; Apenten, R. K. O. Heat-induced denaturation and aggregation of β-lactoglobulin: Kinetics of formation of hydrophobic and disulphide-linked aggregates. *Int. J. Food Sci. Technol.* **1999**, *34*, 467−476.

(14) Tolkach, A.; Kulozik, U. Effect of pH and temperature on the reaction kinetic parameters of the thermal denaturation of β-lactoglobulin. *Milchwissenschaft* **2005**, *60*, 249−252.

(15) de la Fuente, M. A.; Singh, H.; Hemar, Y. Recent advances in the characterisation of heat-induced aggregates and intermediates of whey proteins. *Trends Food Sci. Technol.* **2002**, *13*, 262−274.

(16) Hoffmann, M. A. M.; vanMil, P. Heat-induced aggregation of β-lactoglobulin: Role of the free thiol group and disulfide bonds. *J. Agric. Food Chem.* **1997**, *45*, 2942−2948.

(17) Gotham, S. M.; Fryer, P. J.; Pritchard, A. M. β-Lactoglobulin denaturation and aggregation reactions and fouling deposit formation—A DSC study. *Int. J. Food Sci. Technol.* **1992**, *27*, 313−327.

(18) Elofsson, U. M.; Paulsson, M. A.; Sellers, P.; Arnebrant, T. Adsorption during heat treatment related to the thermal unfolding/aggregation of β-lactoglobulins A and B. *J. Colloid Interface Sci.* **1996**, *183*, 408−415.

(19) Santos, O.; Nylander, T.; Schillen, K.; Paulsson, M.; Tragardh, C. Effect of surface and bulk solution properties on the adsorption of whey protein onto steel surfaces at high temperature. *J. Food Eng.* **2006**, *73*, 174−189.

(20) Tiefenthaler, K.; Lukosz W., Sensitivity of grating couplers as integrated-optical chemical sensors. *J. Opt. Soc. Am. B* **1989**, *6*, 209−220.

(21) Haarmans, M. T.; Bedeaux, D. Optical properties of thin films up to second order in the thickness. *Thin Solid Films* **1995**, *258*, 213−223.

(22) Mann, E. K. Evaluating optical techniques for determining film structure: Optical invariants for anisotropic dielectric thin films. *Langmuir* **2001**, *17*, 5872−5881.

(23) Defeijter, J. A.; Benjamins, J.; Veer, F. A. Ellipsometry as a tool to study the adsorption behavior of synthetic and biopolymers at the air−water interface. *Biopolymers* **1978**, *17*, 1759−1772.

(24) Van Tassel, P. R. Statistical mechanical modeling of protein adsorption. *Materialwiss. Werkstofftech.* **2003**, *34*, 1129−1132.

(25) Szollosi, G. J.; Derenyi, I.; Voros, J. Reversible mesoscopic model of protein adsorption: From equilibrium to dynamics. *Physica A* **2004**, *343*, 359−375.

(26) Saini, S.; Kurrat, R.; Prenosil, J. E.; Ramsden, J. J. Temperature dependence of pyrolysed sol−gel planar waveguide parameters. *J. Phys. D: Appl. Phys.* **1994**, *27*, 1134−1138.

(27) Hoffmann, M. A. M.; Roefs, S.; Verheul, M.; VanMil, P.; DeKruif, K. G. Aggregation of β-lactoglobulin studied by in situ light scattering. *J. Dairy Res.* **1996**, *63*, 423−440.

(28) Verheul, M.; Roefs, S.; de Kruif, K. G. Kinetics of heat-induced aggregation of β-lactoglobulin. *J. Agric. Food Chem.* **1998**, *46*, 896−903.

(29) Law, A. J. R.; Leaver, J. Effect of pH on the thermal denaturation of whey proteins in milk. *J. Agric. Food Chem.* **2000**, *48*, 672−679.

(30) Hunter, R. J. *Foundations of Colloid Science*, 2nd ed.; Oxford University Press: New York, 2001.

(31) Vonhippe, P.; Schleich, T. Ion effects on solution structure of biological macromolecules. *Acc. Chem. Res.* **1969**, *2*, 257−265.

(32) MicroVacuum. *OWLS BioSense 2.2 Software Database*; MicroVacuum: Budapest, Hungary, 2003.

(33) Sefcik, J.; Kroslak, M.; Morbidelli, M. Optical response of porous titania−silica waveguides to surface charging in electrolyte filled pores. *Helv. Chim. Acta* **2002**, *85*, 3508−3515.

BM060293+